Fermi National Accelerator Laboratory

FERMILAB-PUB-91/182-T

June 1991

NEUTRINO MASSES AND MIXINGS BASED ON A SPECIAL SET OF QUARK MASS MATRICES (II)

Carl H. ALBRIGHT

Department of Physics, Northern Illinois University, DeKalb, Illinois 60115*

and

Fermi National Accelerator Laboratory, P.O. Box 500, Batavia, Illinois 60510†

Abstract

In the framework of a 6×6 neutrino mass matrix with the standard seesaw mechanism, simple forms are used for the leptonic Dirac mass submatrices which exhibit hierarchical chiral symmetry-breaking structure with just six parameters, as suggested by our previous work with quark mass matrices. Through a Monte Carlo analysis of Euler angle rotations applied to diagonal forms for the righthanded Majorana mass submatrix, we generate scatter plots in the δm_{23}^2 vs. $\sin^2 2\theta_{23}$ and δm_{13}^2 vs. $\sin^2 2\theta_{13}$ oscillation planes for a fixed point in the nonadiabatic MSW band. While the most probable values in the 23 plane lie ajacent to the present experimentally-excluded region, there are some interesting theoretical cases which are several orders of magnitude removed from it.

PACS numbers: 12.15.Ff, 14.60Gh, 14.80Dq, 96.60Kx

*Permanent address

†Electronic address: ALBRIGHT@FNAL

Operated by Universities Research Association Inc. under contract with the United States Department of Energy

I. INTRODUCTION

Recent data from the LEP and SLC e^+e^- collider experiments[1] have demonstrated beyond all doubt that there are just three families of light leptons, where the lefthanded neutrinos and charged leptons form $SU(2)_L \otimes U(1)_Y$ doublets, while the righthanded charged leptons exist as singlets under the same electroweak group. The number of righthanded neutrino singlets remains completely uncertain, since such objects do not couple to the neutral weak Z^o boson, even if they exist. They will play an important role in the Yukawa part of the Lagrangian, however, as they determine in a crucial way the structure of the neutrino mass matrix, the resulting neutrino mass spectrum and weak mixing angles of the mass eigenstates with respect to the weak flavor states and to the charged leptonic current interactions. Even a fourth heavy family of lefthanded lepton (and quark) doublets is a possibility.

Recent suggestions that neutrinos have small masses compared to the GeV scale, in order to explain the observed solar neutrino deficit[2] in terms of matter-induced neutrino resonant oscillations,[3] must be taken seriously. Moreover, the appearance[4] of a 17 keV neutrino in beta decays observed with solid-state detectors has also helped to focus attention on the neutrino mass issue. In the minimal standard model with no righthanded neutrino singlets, neutrino masses can be generated only through Majorana mass terms involving just the lefthanded doublets in the presence of a Higgs triplet. But such a minimal mechanism can not explain[5] the enhanced solar neutrino nonadiabatic MSW $\nu_e - \nu_\mu$ mixing effect. In order to do so, one must introduce righthanded singlets into the model.

While other possibilities[6] have been explored in connection with the 17 keV neutrino, a rather natural choice is to introduce three righthanded neutrino singlets to parallel the three sets of righthanded charged leptons, and up and down quarks. This is certainly the choice of models based on grand unification involving the unifying groups[7] of $SO(10)$, flipped $SU(5) \times$

$U(1)$, E_6, etc. where an $SU(4)$ subgroup can break according to $SU(4) \to SU(3)_c \otimes U(1)$ with $4 \to \mathbf{3} \oplus \mathbf{1}$ as a lepton emerges for each colored triplet of quarks. In such models, the neutrino Dirac mass submatrices should have forms closely allied with the up quark mass matrix, while the charged lepton mass matrix parallels the down quark mass matrix. In short, the same VEVs apply for the quarks and leptons, at least for the Dirac sectors, though the Yukawa couplings may differ. The lefthanded and righthanded Majorana submatrices which can only arise from couplings to Higgs triplets and singlets, respectively, remain undetermined in the absence of a specific model. If the righthanded Majorana submatrix is rank 3 and has entries $O(M)$ where $M \gg m_l$, a typical lepton mass, this class of models exhibits the well-studied seesaw mechanism.[8] This enables one to understand easily why the light neutrino masses are $O(m_l^2/M)$, so much smaller than their charged lepton counterparts. However, if the righthanded Majorana submatrix is rank 2 or less, the seesaw mechanism is incomplete,[9] and one or more pairs of Dirac (or pseudo-Dirac) neutrinos are generated.

In order to investigate the neutrino masses and mixings which arise due to the quarklike forms for the Dirac submatrices, one must adopt some model or empirical form for the quark mass matrices. Although the precise form of the quark mass matrices is not known, the principle of hierarchical chiral symmetry breaking advanced years ago by Fritzsch[10] seems to play an important role, as all the hadronic charged-current constraints on the Cabibbo-Kobayashi-Maskawa[11] (CKM) mixing matrix and higher-order flavor-changing processes can be well satisfied in this framework. A set of particularly simple empirical matrices[12] which works in the neighborhood of a top quark mass near 130 - 135 GeV was used by the author[13] in (I) for the Dirac submatrices; the righthanded Majorana matrix was chosen to be diagonal for simplicity. Here we shall discuss the model and results in somewhat more detail and perform a Monte Carlo analysis on Euler rotations of the diagonal righthanded Majorana matrix, so as to determine the full range of solutions in the δm_{ij}^2 vs. $\sin^2 2\theta_{ij}$ neutrino

oscillation planes.

We note in passing that attempts[14] to generate a 17 keV Dirac neutrino in the above framework with a rank 2 righthanded Majorana submatrix generally fail to satisfy all the experimental constraints. The Dirac submatrices apparently must involve a very different Higgs mechanism than that for the quarks and charged leptons. In particular, the model that Babu and Mohapatra[15] constructed is definitely non-hierarchical in texture.

In Section II we discuss the empirical forms of the quark mass matrices we shall adopt for the leptonic Dirac submatrices. The results obtained in Section III apply for diagonal righthanded Majorana submatrices. In Section IV we perform Euler rotations on the diagonal Majorana submatrices and obtain the preferred regions in the δm^2_{ij} vs. $\sin^2 2\theta_{ij}$ neutrino oscillation planes. A summary of the results is presented in Section V.

II. EMPIRICAL QUARK MASS MATRICES

The Fritzsch[10] quark mass matrices based on hierarchical chiral symmetry breaking

$$\mathbf{M_U} = \begin{pmatrix} 0 & A & 0 \\ A & 0 & B \\ 0 & B & C \end{pmatrix}, \qquad \mathbf{M_D} = \begin{pmatrix} 0 & A' & 0 \\ A'^* & 0 & B' \\ 0 & B'^* & C' \end{pmatrix} \tag{2.1}$$

have served as a standard set for over twelve years since they were introduced. It is generally recognized,[16] however, that the increased accuracy with which the Cabibbo-Kobayashi-Maskawa[11] (CKM) mixing matrix elements are now known has limited the utility of the matrices to top quark masses $m_t \lesssim 100 - 110$ GeV. Experimentally the present lower bound on m_t is conservatively placed at 89 GeV by the CDF collaboration[17] at Fermilab.

Bearing this in mind, the author[12] sometime ago made a more general search of quark mass matrices which exhibit hierarchical chiral symmetry breaking but admit top quark

masses higher than attainable with the Fritzsch matrices. For this purpose, the following forms were adopted

$$\mathbf{M}_U = \begin{pmatrix} 0 & A & D \\ A & E & B \\ D^* & B & C \end{pmatrix}, \qquad \mathbf{M}_D = \begin{pmatrix} 0 & A' & D' \\ A'^* & E' & B' \\ D'^* & B'^* & C' \end{pmatrix} \tag{2.2a}$$

with the explicitly assumed relaxed hierarchies

$$\begin{aligned} 0 << |A|,\ |E|,\ \ |D| << |B| << |C| \\ 0 << |A'|,\ |E'|,\ \ |D'| << |B'| << |C'| \end{aligned} \tag{2.2b}$$

in an effort to determine the allowed top quark mass spectrum. There are now 14 parameters, 10 amplitudes and 4 phase angles, in place of Fritzsch's 8 parameters to explain the 6 quark masses, 3 mixing angles and 1 mixing phase. The complexity of the computer search was reduced by choosing to ignore the small u-quark mass by taking $E = A = 0$ and D real. A perturbation about the results obtained *a postieri* justified this procedure. The key feature which admits higher top quark mass solutions consistent with the experimental constraints was found to be the nonvanishing diagonal elements, E and E', expecially the latter.

The search method employed then consisted of the following steps:[12]

(1) Pick a top quark mass and vary the free mass matrix parameters. All mixing matrix elements $|(V_{CKM})_{ij}|$ are required to fit the experimental values determined by Schubert[18] to within one standard deviation accuracy.

(2) The commutator determinant of the mass matrices is used to compute the Jarlskog J-value[19] from which $\sin\delta$ can be determined with the help of the $|(V_{CKM})_{ij}|$. The first-second quadrant ambiguity for the CP-violating phase δ is taken into account.

(3) Additional constraints were imposed on the following parameters:

$$\begin{aligned} 0.07 &\leq |V_{ub}/V_{cb}| \leq 0.15 \\ 1.3 &\leq |V_{td}^* V_{tb}|^2 S \simeq (1.8 \pm 0.3)\frac{(0.140)^2}{B_B F_B^2} \leq 2.3 \\ 0.55 &\leq B_K \leq 0.90 \end{aligned}$$

where B_B and B_K are the B and K meson bag parameters, F_B is the B meson decay constant and S is a radiative correction factor.

(4) The procedure is repeated for different m_t.

Two peaks occur in the top quark mass probability distribution, especially for $\cos\delta > 0$, which correspond to $m_t = 135 \pm 25$ GeV and $m_t = 300 \pm 100$ GeV for a strange quark mass of $m_s(1\text{GeV}) = 120$ MeV, with the lower peak strongly preferred. The results obtained from this quark mass matrix approach are in good agreement with other analyses such as that by Kim, Rosner and Yuan[20] which use the approximate Wolfenstein parametrization[21] of the mixing data and present chi-square contours in the η *vs.* m_t plane, where η is one of the Wolfenstein parameters. Although one can not rule out a very massive top quark with $m_t \gg 200$ GeV on the basis of the flavor-changing data alone, the most probable value of 135 GeV is in good agreement with that deduced from the neutral-current data by Langacker, Ellis and Fogli, and others.[22]

A careful, but not exhaustive, search for a viable alternative to the Fritzsch model was also carried out. One special empirical model was found which fits all the data remarkably well with a top quark mass in the narrow range from 130 to 140 GeV - at the very peak of the mass spectrum - and is described by the following set of quark mass matrices:[12]

$$\mathbf{M}_U = \begin{pmatrix} 0 & A_U & A_U \\ A_U & A_U & B_U \\ A_U & B_U & C_U \end{pmatrix}, \qquad \mathbf{M}_D = \begin{pmatrix} 0 & iA'_D & -A'_D \\ -iA'_D & -A'_D & B'_D \\ -A'_D & B'_D & C'_D \end{pmatrix} \tag{2.3}$$

with just 6 real parameters ordered according to $A_U \ll B_U \ll C_U$, $A'_D \ll B'_D \ll C'_D$. With $m_s(1\text{GeV}) = 120$ MeV again chosen and $m_t = 133$ GeV, these matrices lead to a CKM mixing matrix which lies well within the experimental errors assigned by Schubert and to the results $|V_{ub}/V_{cb}| = 0.72$, $|V_{td}^* V_{tb}|^2 S = 1.32$ corresponding to $x_d = 1.7$, $B_K = 0.78$ for the bag parameter in K decay, and $\epsilon'/\epsilon \simeq 0.77 \times 10^{-3}$. For $m_s(1\text{GeV}) = 130$ MeV, the preferred value for the top quark mass drops to 125 MeV.

In what follows we shall make use of these simple empirical forms of the quark mass matrices for the leptonic Dirac sector. The clear advantage is that they represent the most probable top quark mass extremely well and involve so few parameters, six instead of eight for the Fritzsch model. This will greatly aid in our analysis of the neutrino situation, where one must assign extra parameters to the Majorana submatrices.

III. APPLICATION TO LEPTONS WITH DIAGONAL $\mathbf{R}_M$

We now extend our analysis to the lepton mass matrices as suggested by grand unified models[7] based on $SO(10)$, flipped $SU(5) \times U(1)$, $SU(15)$, E_6 and the like, in order to compute neutrino masses and mixings. For this purpose, we first note that with three lefthanded neutrinos tranforming as members of $SU(2)_L \times U(1)_Y$ doublets and three righthanded neutrino singlets, we must deal with 6×6 matrices. In terms of the weak flavor bases $\overline{B_L} = \{\overline{\nu'_{iL}}, \overline{(\nu_i'^c)_L}\}$, $B_R = \{(\nu_i'^c)_R, \nu'_{iR}\}$ and likewise for the charged leptons, the mass matrices have the following general complex symmetric forms

$$M_N = \begin{pmatrix} \mathbf{L}_M & \mathbf{M}_N \\ \mathbf{M}_N^T & \mathbf{R}_M \end{pmatrix}, \qquad M_L = \begin{pmatrix} 0 & \mathbf{M}_L \\ \mathbf{M}_L^T & 0 \end{pmatrix} \tag{3.1}$$

for neutrinos and charged leptons, respectively. Here $\mathbf{M}_N$ and $\mathbf{M}_L$ are the Dirac mass submatrices, and $\mathbf{L}_M$ and $\mathbf{R}_M$ are the lefthanded and righthanded Majorana neutrino mass

submatrices.

From here on we shall assume that the leptonic Dirac submatrices $\mathbf{M}_N$ and $\mathbf{M}_L$ have the same forms as the quark matrices $\mathbf{M}_U$ and $\mathbf{M}_D$, respectively, in (2.3) under the assumption that the same Higgs doublet couples to $\mathbf{M}_N$ and $\mathbf{M}_U$, and likewise for $\mathbf{M}_L$ and $\mathbf{M}_D$:

$$\mathbf{M}_N = \begin{pmatrix} 0 & A_N & A_N \\ A_N & A_N & B_N \\ A_N & B_N & C_N \end{pmatrix}, \qquad \mathbf{M}_L = \begin{pmatrix} 0 & iA'_L & -A'_L \\ -iA'_L & -A'_L & B'_L \\ -A'_L & B'_L & C'_L \end{pmatrix} \tag{3.2}$$

We allow the particular values of A_N and A_U, and A'_L and A'_D, to differ since the Yukawa couplings for the neutrinos and up quarks, and likewise charged leptons and down quarks, need not be the same. In the absence of Higgs triplets, which we shall conventionally assume,[23] $\mathbf{L}_M$ is the zero matrix since the lefthanded doublets couple to form a symmetric $SU(2)_L$ triplet state; on the other hand, the righthanded Majorana neutrino mass terms in $\mathbf{R}_M$ can arise from couplings to Higgs singlets or from bare mass terms in the fundamental Lagrangian. For simplicity and a first look in this Section, we shall take $\mathbf{R}_M$ to be diagonal, as done in (I),[13] and equal to

$$\mathbf{D}_M = diag(D_1,\ D_2,\ D_3) \tag{3.3}$$

The neutrino mass matrix then has the simple form

$$M_N = \begin{pmatrix} 0 & \mathbf{M}_N \\ \mathbf{M}_N^T & \mathbf{D}_\mathbf{M} \end{pmatrix} \tag{3.4}$$

The matrices in the weak bases in (3.4) and (3.1) are related to those in the mass bases by

$$M_N = U_L^\dagger D_N U_R, \qquad \mathbf{M}_L = U_L'^\dagger \mathbf{D}_L U'_R \tag{3.5a}$$

in terms of the four unitary transformation matrices U_L, U_R, U'_L and U'_R, and the diagonal

mass matrices

$$D_N = diag(\lambda_1,\ \lambda_2,\ \lambda_3,\ \lambda_4,\ \lambda_5,\ \lambda_6), \qquad \mathbf{D}_L = diag(\lambda'_1,\ \lambda'_2,\ \lambda'_3) \tag{3.5b}$$

where the λ_α and λ'_j are the neutrino and charged lepton masses up to a sign. The charged-current interactions involve just the lefthanded neutrinos and charged leptons in the weak bases

$$\mathcal{L}_W^{(\pm)} = -g\overline{\nu'_{iL}}\gamma^\mu \ell'_{iL} W_\mu + h.c. \tag{3.6a}$$

In terms of the mass eigenbases,

$$\mathcal{L}_W^{(\pm)} = -g\overline{\nu_{\alpha L}}\gamma^\mu (V_{CKM})_{\alpha j}\ell_{jL} + h.c. \tag{3.6b}$$

so the counterpart of the quark CKM matrix is 6×3 and given by

$$(V_{CKM})_{\alpha j} = (U_L)_{\alpha i}(U'^\dagger_L)_{ij}, \qquad \alpha = 1-6; \quad i,j = 1,2,3 \tag{3.6c}$$

under the assumption that there are 6 neutrino mass states but just 3 charged lepton mass states in the $SU(2)_L \times U(1)_Y$ electroweak theory.

In order to calculate the squares of the mixing matrix elements, we generalize the projection operator technique of Jarlskog[24] and find

$$|(V_{CKM})_{\alpha j}|^2 = \mathrm{Tr}\left[P_\alpha P'_j\right] = (P_\alpha)_{kl}(P'_j)_{lk} \tag{3.7a}$$

where

$$P_\alpha = U_L^\dagger P^D U_L = \prod_{\gamma\neq\alpha}(\lambda_\gamma \mathbf{I} - M_N)/\prod_{\delta\neq\alpha}(\lambda_\delta - \lambda_\alpha) \tag{3.7b}$$

$$P'_j = U'^\dagger_L P'^D U'_L = \prod_{k\neq j}(\lambda'_k \mathbf{I} - \mathbf{M}_L)/\prod_{l\neq j}(\lambda'_l - \lambda'_j) \tag{3.7c}$$

and P^D and P'^D are the diagonal projection operators. In writing these expressions, we have explicitly made use of the fact that our matrices M_N and $\mathbf{M}_L$ are Hermitian, so that we can take $U_R = U_L$ and $\mathbf{U}'_R = \mathbf{U}'_L$ to diagonalize the matrices. The trace expressions are calculated analytically through use of MACSYMA and then evaluated numerically in a FORTRAN program. To achieve sufficient accuracy (1 part in 10^5), we have used quadruple precision on a VAX computer to calculate the mass eigenvalues λ_α and λ'_j from the characteristic equations.

We begin our search for the neutrino masses and mixings allowed in our model by determining the charged lepton parameters in (3.2) uniquely to be

$$A'_L = 0.007576, \qquad B'_L = 0.4181, \qquad C'_L = 1.686 \text{ GeV} \tag{3.8a}$$

from the known charged lepton masses and the invariant properties of the traces and determinant relative to the weak and mass eigenbases. By way of comparison, we note that for the special set of quark mass matrices in (2.2) with $m_t = 133$ GeV giving the best fit to the flavor-changing data, the 6 parameters in $\mathbf{M}_U$ and $\mathbf{M}_D$ are determined at 1 GeV to be

$$\begin{aligned} A_U &= 0.0755, \qquad B_U = 17.54, \qquad C_U = 213.6 \text{ GeV} \\ A'_D &= 0.0274, \qquad B'_D = 0.6782, \qquad C'_D = 5.214 \text{ GeV} \end{aligned} \tag{3.8b}$$

If we neglect the small running effect of the Yukawa couplings, the charged lepton and down quark parameters are scaled by

$$A'_D/A'_L = 3.62, \qquad B'_D/B'_L = 1.62, \qquad C'_D/C'_L = 3.09 \tag{3.8c}$$

For point of reference then, we note that the neutrino parameters scaled in the same fashion would be given by

$$A_N = 0.0209, \qquad B_N = 10.83, \qquad C_N = 69.13 \text{ GeV} \tag{3.8d}$$

The Majorana entries in $\mathbf{R}_M$, which we have assumed here to be diagonal and equal to $\mathbf{D}_M$, remain completely undetermined; however, the well-known seesaw effect[8] for the neutrino mass matrix M_N implies that if all entries in $\mathbf{M}_N$ are increased by a factor of 10 and the diagonal entries in $\mathbf{D}_M$ are increased by a factor of 100, the light neutrino masses remain unchanged. Moreover, the mixing matrix elements $V_{\alpha j}$ are unchanged. Thus in our search of solutions for the masses and mixing angles, we have the freedom to fix $C_N = 69.13$ as in (3.8d) above and to vary only A_N, B_N and all three D_i.

Our first important observation is that the mixing element $V_{12} \equiv V_{\nu_e \mu}$ is totally insensitive to the choice of the D_i's over an extremely large range. Thus contours can be drawn in the A_N/C_N vs. B_N/C_N plane for fixed $|V_{12}|$ as shown in Fig. 1. In fact, we find a ***minimum*** value of $|V_{12}|$ such that

$$\sin^2 2\theta_{12} \sim 4|V_{12}|^2 \geq 0.0193 \tag{3.9}$$

The acceptable region in this parameter space is bounded by the closely-spaced dotted curve within which the hierarchical conditions

$$0 < |A_N/C_N| \lesssim 0.2|B_N/C_N| \lesssim 0.04 \tag{3.10}$$

are satisfied. Our model, based on the structure of the quark mass matrices, loses much of its credibility if these conditions are badly violated.

While the parameter space of Fig. 1 is highly model-dependent, we mention in passing that in the Fritzsch model no such lower bound on $|V_{12}|^2$ is obtained, if one allows the phase angle $\phi_{A'}$ in (2.1) to run down to 0°; however, the Fritzsch model can remotely fit the quark data only[16] if $\phi_{A'}$ lies in the range $80^\circ \lesssim \phi_{A'} \lesssim 100^\circ$. For these values, the lower bound in (3.9) also applies approximately.

This lower bound has interesting implications for the expected solar neutrino capture

rates in the experimentally preferred nonadiabatic Mikheyev, Smirnov and Wolfenstein[3] (MSW) region, whereby one can understand the observed depletion of the solar neutrino flux due to resonant oscillations as the emitted neutrinos pass through the dense solar matter. In Fig. 2 we show the allowed MSW region bounded by the dotted curves and the gallium solar neutrino capture rate contours (isoSNUs), as calculated by Parke and Walker.[25] The lower bound on $|V_{12}|^2$, as indicated by the dotted vertical line at $4\sin^2\theta_{12} = 0.0193$, translates into a maximum capture rate in gallium of about 25 SNU in the nonadiabatic region along the hypotenuse of the triangular-shaped region. From the work of Bahcall and Haxton,[26] who have considered a much wider range of solar models, the upper bound on the gallium solar neutrino capture rate can be as high as 40 SNU. The preliminary data from the SAGE experiment[27] are quite consistent with these observations.

We now fix $|V_{12}|^2 \simeq \sin^2\theta_{12} = 0.00485$ and adjust $\delta m^2_{12} \equiv m^2_{\nu_2} - m^2_{\nu_1}$ so that the point lies in the narrow allowed nonadiabatic MSW band in Fig. 2 corresponding to[28]

$$\delta m^2_{12}\sin^2\theta_{12} = 1.0 \times 10^{-8}\ \mathrm{eV}^2 \tag{3.11}$$

i.e., $\delta m^2_{12} \simeq 2.06 \times 10^{-6}\ \mathrm{eV}^2$. If we do this by taking all D_i's comparable while moving upward along the fixed $|V_{12}|^2 = 0.00485$ contour in the A_N/C_N vs. B_N/C_N plane of Fig. 1, we traverse in a downward direction the solid curve in the δm^2_{23} vs. $\sin^2 2\theta_{23}$ plane in Fig. 3(a). In fact, we can explore the dependence of δm^2_{23} and $\sin^2 2\theta_{23}$ on the parameters D_i, for the same point ($|V_{12}|^2 = 0.00485$, $\delta m^2_{12} = 2.06 \times 10^{-6}\ \mathrm{eV}^2$) in the MSW band of (3.11) by

running along the same contour in Fig. 1 for the following Majorana neutrino cases

$$\begin{array}{lll} (a) & D_1 = 10^2 D_2 = 10^4 D_3 & \text{(upper dot} - \text{dashed curve)} \\ (b) & D_1 = 10 D_2 = 10^2 D_3 & \text{(upper dashed curve)} \\ (c) & D_1 \sim D_2 \sim D_3 & \text{(solid curve)} \\ (d) & 10^2 D_1 = 10 D_2 = D_3 & \text{(lower dashed curve)} \\ (e) & 10^4 D_1 = 10^2 D_2 = D_3 & \text{(lower dot} - \text{dashed curve)} \end{array} \tag{3.12}$$

where the description for each case pertains to the curves in Fig. 3(a). The closely-spaced dotted curves represent the present experimental upper bounds from the E531 experiment[29] at Fermilab and CDHSW[30] at CERN. The allowed region of interest lies between these experimental curves and the dotted curve obtained from the locus of points for which the hierarchy condition $B_N/C_N < 0.20$ in (3.10) is satisfied. For the choice of parameters selected in (3.12), there is a very narrow allowed band lying along $\sin^2 2\theta_{23} = 0.0037$ with a tau neutrino mass in the range $12 \lesssim m_{\nu_\tau} \lesssim 120$ eV. The considerably larger allowed region occurs with $0.15 \lesssim m_{\nu_\tau} \lesssim 5$ eV, and $0.004 \lesssim \sin^2 2\theta_{23} \lesssim 0.16$. The points indicated by crosses in Fig. 3(a) correspond to the special set of parameters A_N, B_N and C_N given in (3.8d) for which $|V_{12}|^2 = 0.00488$ with the D_i's adjusted to give $\delta m_{12}^2 = 2.05 \times 10^{-6}$ eV^2 in the nonadiabatic MSW band of (3.11). The corresponding allowed region in the δm_{13}^2 vs. $\sin^2 2\theta_{13}$ plane is not shown here, but lies in a narrow band centered around $\sin^2 2\theta_{13} = 10^{-4}$.

In Fig. 3(b) the results are presented for the point ($|V_{12}|^2 = 0.05$, $\delta m_{12}^2 = 2.0 \times 10^{-7}$ eV^2) in the MSW band, where the running occurs along the upper dot-dashed contour in Fig. 1. Note that the allowed region is somewhat distorted from that appearing in Fig. 3(a). The required hierarchy conditions (3.11) are not satisfied here for cases (d) and (e) of (3.12) above.

It is of some interest to exhibit the mixing matrix that emerges for two special, but typical,

cases. The projection operator technique employed enables us to calculate independently the squares of all 18 elements as displayed below. For the following choice of parameters

$$\begin{aligned} &A_N = 0.06 \text{ GeV}, \; B_N = 14.0 \text{ GeV}, \; C_N = 69.1 \text{ GeV} \\ &D_1 = 5.16 \times 10^{14} \text{ GeV}, \; D_2 = 5.16 \times 10^{12} \text{ GeV}, \; D_3 = 5.16 \times 10^{10} \text{ GeV} \end{aligned} \tag{3.13a}$$

corresponding to the left-most point on the upper dot-dashed curve of Fig. 3(a), we obtain for the light neutrino masses

$$m_1 = 1.16 \times 10^{-12} \text{ eV}, \qquad m_2 = 1.44 \times 10^{-3} \text{ eV}, \qquad m_3 = 96.4 \text{ eV} \tag{3.13b}$$

with the heavy ones being equal to D_3, D_2, and D_1 in increasing order; the squares of the mixing matrix elements are

$$|V_{\alpha j}|^2 = \begin{pmatrix} 0.99513 & 0.00485 & 0.00002 \\ 0.00484 & 0.99429 & 0.00087 \\ 0.00003 & 0.00086 & 0.99911 \\ 0.55 \times 10^{-18} & 0.16 \times 10^{-16} & 0.19 \times 10^{-13} \\ 0.22 \times 10^{-22} & 0.37 \times 10^{-20} & 0.70 \times 10^{-19} \\ 0.39 \times 10^{-30} & 0.75 \times 10^{-28} & 0.20 \times 10^{-27} \end{pmatrix} \tag{3.13c}$$

On the other hand for a second set of parameters yielding the point marked with a cross on the dashed line of Fig. 3(a)

$$\begin{aligned} &A_N = 0.03 \text{ GeV}, \; B_N = 10.8 \text{ GeV}, \; C_N = 69.1 \text{ GeV} \\ &D_1 = 1.52 \times 10^{11} \text{ GeV}, \; D_2 = 1.52 \times 10^{12} \text{ GeV}, \; D_3 = 1.52 \times 10^{13} \text{ GeV} \end{aligned} \tag{3.14a}$$

we obtain for the light neutrino masses

$$m_1 = 9.15 \times 10^{-10} \text{ eV}, \qquad m_2 = 1.44 \times 10^{-3} \text{ eV}, \qquad m_3 = 0.40 \text{ eV} \tag{3.14b}$$

with the heavy ones being equal to D_1, D_2, and D_3 in increasing order; the squares of the mixing matrix elements are

$$|V_{\alpha j}|^2 = \begin{pmatrix} 0.99514 & 0.00485 & 0.00002 \\ 0.00478 & 0.98457 & 0.01064 \\ 0.00008 & 0.01058 & 0.98934 \\ 0.11 \times 10^{-25} & 0.22 \times 10^{-23} & 0.56 \times 10^{-23} \\ 0.14 \times 10^{-23} & 0.25 \times 10^{-21} & 0.48 \times 10^{-20} \\ 0.10 \times 10^{-24} & 0.12 \times 10^{-22} & 0.21 \times 10^{-20} \end{pmatrix} \tag{3.14c}$$

From the above, we easily see that all three columns of each matrix individually sum to unity, as must be the case since a given flavor state is a linear combination of mass eigenstates with unit norm. The first three rows also sum to unity, as only these three mass eigenstates participate in the lefthanded weak interactions; the fourth, fifth and sixth mass eigenstates with heavy masses are effectively decoupled from the weak interactions. Hence the mixing matrices are essentially 3 x 3, and all neutrino mass eigenstates are of the Majorana type. The "unitary" nature of (3.13c) and (3.14c) provides an excellent numerical check on our procedure.

While $|V_{12}|$ is independent of D_1, D_2 and D_3; V_{23} does depend on these values as seen in (3.13c) and (3.14c) above. The clear suggestion from our work in this Section is that much of the theoretically-allowed region in the δm_{23}^2 vs. $\sin^2 2\theta_{23}$ plane has been excluded by the present experimentally-forbidden region. Hence much effort should be made to restrict the allowed region even further. In the next Section where we consider nondiagonal forms of the Majorana submatrix $\mathbf{R}_M$, we shall see that this striking conclusion is weakened to some extent.

IV. MONTE CARLO ANALYSIS FOR NONDIAGONAL $\mathbf{R}_M$

We now wish to consider the more general situation where the righthanded Majorana submatrix $\mathbf{R}_M$ is nondiagonal. Since $\mathbf{R}_M$ has the following structure in flavor space with Φ a Higgs singlet

$$(\mathbf{R}_M)_{ij} = \overline{(\nu_i'^c)_L}\nu'_{jR}\Phi = \nu_{iR}'^T C \nu'_{jR}\Phi \tag{4.1}$$

it can be chosen real symmetric and diagonalized by an orthogonal transformation. This suggests that we can use our previous analysis in Section III and simply rotate the diagonal $\mathbf{D}_M$ in order to obtain the nondiagonal form

$$\mathbf{R}_M = R^T(\alpha,\beta,\gamma)\mathbf{D}_M R(\alpha,\beta,\gamma) \tag{4.2}$$

Hence we can consider each one of the five cases in (3.12) and perform this Euler rotation. Of course, for case (3.12c) which is proportional to the unit matrix, the rotated $\mathbf{D}_M$ remains unchanged, so the solid curves in Figs. 3(a,b) remain unchanged.

In order to handle the other four cases in a meaningful way, we shall concentrate on the case $|V_{12}|^2 = 0.00485$ illustrated in Fig. 3(a) and proceed as follows. We select three points along each of the dashed and dot-dashed curves in Fig. 3(a) which lie in the physically-interesting hierarchical region for which

$$(B_N/C_N, A_N/C_N) = \begin{cases} (0.0868,\ 1.45\times 10^{-4}) \\ (0.156,\ 4.34\times 10^{-4}) \\ (0.203,\ 8.68\times 10^{-4}) \end{cases} \tag{4.3}$$

These points on the four curves are indicated by crosses in Fig. 4(a), while the corresponding points of the solid curve of Fig. 3(a) are indicated with cross potents. For each one of these points we perform Euler angle rotations of the corresponding diagonal righthanded Majorana submatrix $\mathbf{D}_M$. While the value of $|V_{12}|^2$ is unaffected by such rotations, we must rescale

the D_i's, so that the point in the MSW band at ($|V_{12}|^2 = 0.00485$, $\delta m^2_{12} = 2.06 \times 10^{-6}$ eV^2) is retained after each rotation. In order to cover the full Euler angle parameter space, we have used a Monte Carlo analysis, whereby 5000 random Euler angle rotation matrices are applied in turn to each point singled out. The region in the δm^2_{23} vs. $\sin^2 2\theta_{23}$ plane is binned, and the numbers of points in each bin arising from all 60,000 rotations are presented as a scatter plot in Fig. 4(a). This same procedure is used to obtain a scatter plot for the δm^2_{13} vs. $\sin^2 2\theta_{13}$ plane in Fig. 4(b).

The results obtained are rather puzzling. While most of the points resulting from the rotation of $\mathbf{D}_M$ remain inside the original boundary indicated now by a dot-dashed line in Fig. 4(a), some points are randomly distributed several orders of magnitude outside this boundary. The resultant spread of points in the δm^2_{13} vs. $\sin^2 2\theta_{13}$ plane of Fig. 4(b), however, is considerably more constrained.

In order to illustrate the types of nondiagonal $\mathbf{R}_M$ which lead to these atypical points, we have starred two points labeled A and B in Fig. 4 and present their particular $\mathbf{R}_M$ below, where the smallest nonvanishing entries are normalized to unity:

$$\text{Point A}: \qquad \mathbf{R}_M = \begin{pmatrix} 2.9 & 2.0 & 1.4 \\ 2.0 & 2.0 & 1.3 \\ 1.4 & 1.3 & 1 \end{pmatrix} \tag{4.4a}$$

$$\text{Point B}: \qquad \mathbf{R}_M = \begin{pmatrix} 0 & 1 & 1 \\ 1 & 1 & 100 \\ 1 & 100 & 1000 \end{pmatrix} \tag{4.4b}$$

For point A, $\mathbf{R}_M$ was obtained by a simple rotation of $\mathbf{D}_M$ with the diagonal entries scaled as in case (b) of (3.12), while $\mathbf{R}_M$ for point B was constructed to give a hierarchical form by fiat. Of course both matrices must be scaled accordingly in order to obtain the desired MSW point in the δm^2_{12} vs. $\sin^2 2\theta_{12}$ plane. The third set of values for (B_N/C_N, A_N/C_N)

in (4.3) was used for points A and B.

The righthanded Majorana submatrix $\mathbf{R}_M$ for point A exhibits an inverted hierarchy with *nonincreasing* entries as one moves from one skew diagonal to another. By inspection of many other cases, we find that other $\mathbf{R}_M$ with inverted hierarchies which do not have this property yield points which lie within the original boundary in Fig. 3(a). The form of $\mathbf{R}_M$ for point B is of some interest, for it exhibits somewhat the same hierarchy as the Dirac submatrix $\mathbf{M}_N$ in (3.2).

V. SUMMARY

We have started from a grand-unified-type model with three families of quark and lepton lefthanded doublets and a set of three righthanded neutrino singlets to parallel the three sets of righthanded quark and charged-lepton singlets. The Dirac mass submatrices for the neutrinos and charged leptons are chosen to have the same forms as those associated with the up and down quarks, respectively. For this purpose we used a simple set of mass matrices, exhibiting the hierarchical chiral symmetry-breaking structure with just six parameters, which we have shown earlier to work well for quarks if the top quark mass is near 130 - 135 GeV as preferred by the neutral-current and flavor-changing data. In the absence of Higgs triplets, only the righthanded Majorana submatrix $\mathbf{R}_M$ remains completely undetermined. We chose here to ignore the possible existence of a 17 keV neutrino and to consider only rank three $\mathbf{R}_M$'s so the standard seesaw mechanism generates light Majorana neutrinos.

We then proceeded with a phenomenological analysis which first considered only diagonal forms for $\mathbf{R}_M$ and then extended it to nondiagonal $\mathbf{R}_M$ through a Monte Carlo analysis involving Euler angle rotations. In the process, we find a lower bound on $\sin^2 2\theta_{12}$ which translates into an upper bound of 25 - 40 SNU for the solar neutrino capture rate in gallium,

provided the nonadiabatic MSW effect is the correct interpretation for the observed solar neutrino flux deficit.

With regards to the δm_{23}^2 vs. $\sin^2 2\theta_{23}$ oscillation plane, it is clear from our study that while the most probable values, in a purely statistical sense, lie close to the present experimentally-excluded region, there are many atypical points several orders of magnitude removed which may, in fact, be selected by Nature corresponding to some quite reasonable theoretical choices. In the absence of a strong theoretical basis or other important experimental information, we must await the experimental discovery of $\nu_\mu \leftrightarrow \nu_\tau$ and possibly $\nu_e \leftrightarrow \nu_\tau$ oscillations to narrow the theoretical possibilities.

Finally it should be emphasized that, while our whole analysis has been based on the particular forms of $\mathbf{M}_N$ and $\mathbf{M}_L$ given in (3.2), a few spot checks with the Fritzsch forms indicates that our results are not strongly dependent on the choice in (3.2). Our results reflect more importantly on the basic assumption that the hierarchical forms for the quark and lepton mass matrices are closely related in the Dirac sector.

ACKNOWLEDGEMENTS

The author has benefitted from many useful conversations with William A. Bardeen, Stephen J. Parke and N. William Reay, as well as a communication with John N. Bahcall. The author also acknowledges the kind hospitality of the Fermilab Theoretical Physics Department. This research was supported in part by Grant No. PHY-8907806 from the National Science Foundation. Fermilab is operated by Universities Research Association, Inc. under contract with the United States Department of Energy.

References

[1] D. Decamp et al. (ALEPH Collab.), Phys. Lett. B **235**, 399 (1990); M. Z. Akrawy et al. (OPAL Collab.), Phys. Lett. B **240**, 497 (1990); P. Aarnio et al. (DELPHI Collab.), Phys. Lett. B **241**, 425 (1990); B. Adeva et al. (L3 Collab.), Phys. Lett. B **249**, 341 (1990).

[2] R. Davis et al., Phys. Rev. Lett. **20**, 1205 (1968); in *Neutrino '88*, ed. J. Schnepp et al. (World Scientific, 1988); K. Hirata et al., Phys. Rev. Lett. **65**, 1297, 1301 (1990).

[3] S. P. Mikheyev and A. Yu Smirnov, Sov. J. Nucl. Phys. **42**, 913 (1986); Sov. Phys. JETP **64**, 4 (1986); Nuovo Cimento **9C**, 17 (1986); L. Wolfenstein, Phys. Rev. D **17**, 2369 (1978); Phys. Rev. D **20**, 2634 (1979).

[4] J. J. Simpson, Phys. Rev. Lett. **54**, 1891 (1985); J. Simpson and A. Hime, Phys. Rev. D **39**, 1825 (1989); A. Hime and J. J. Simpson, Phys. Rev. D **39**, 1837 (1989); B. Sur et al., Phys. Rev. Lett. **66**, 2444 (1991); A. Hime and N. A. Jelley, Phys. Lett. B **257**, 441 (1991); I. Zlimen et al., Zagreb preprint 11-9/90 LEI.

[5] Y. Zeldovich, DAN SSSR **86**, 505 (1952); E. Konopinsky and H. Mahmoud, Phys. Rev. **92**, 1045 (1953); R. Barbieri and L. J. Hall, Berkeley preprint UCB-PTH-91-13, to be published.

[6] Cf., E. Carlson and L. Randall, Phys. Rev. Lett. **66**, 2947 (1991).

[7] R. Johnson, S. Ranfone and J. Schechter, Phys. Lett. **179B**, 355 (1986); G. Lazarides and Q. Shafi, ICTP preprint IC-90-153; I. Antoniadis, J. Ellis, J. S. Hagelin and D. V. Nanopoulos, Phys. Lett.B **231**, 65 (1989); P. H. Frampton and B.-H. Lee, Phys. Rev. Lett. **64**, 619 (1990).

[8] M. Gell-Mann, P. Ramond and R. Slansky, in "Supersymmetry," edited by P. Van Nieuwenhuizen and D. Z. Freedman (North Holland, 1979); T. Yanagida, Prog. Theor. Phys. B **315**, 66 (1978).

[9] S. L. Glashow, Phys. Lett. B **256**, 218 (1991); M. Fukugita and T. Yanagida, Phys. Rev. Lett. **66**, 2705 (1991).

[10] H. Fritzsch, Phys. Lett. **70B**, 436 (1977); **73B**, 317 (1978); **166B**, 423 (1986).

[11] N. Cabibbo, Phys. Rev. Lett. **10**, 531 (1963); M. Kobayashi and T. Maskawa, Prog. Theor. Phys. **49**, 652 (1973).

[12] C. H. Albright, Phys. Lett. B **246**, 451 (1990); Fermilab preprint FERMILAB-CONF-90/104-T submitted to the XXV International High Energy Physics Conference, Singapore (1990); Fermilab preprint FERMILAB-CONF-90/196-T, to appear in Proceedings of the XXV Int. HEP Conf., Singapore (1990); and references contained therein.

[13] C. H. Albright, Phys. Rev. D **43**, R3595 (1991). We shall henceforth refer to this as (I).

[14] C. H. Albright, Fermilab preprint FERMILAB-PUB-91/29-T, to be published; E. Ma, U. of California at Riverside preprint, UCRHEP-T77(1991), to be published.

[15] K. S. Babu and R. N. Mohapatra, University of Maryland preprint University of Maryland preprint UMD-PP-91-156, to be published.

[16] C. H. Albright, Phys. Lett. B **227**, 171 (1989).

[17] F. Abe et al. (CDF Collab.), Phys. Rev. D **43**, 664 (1991).

[18] K. R. Schubert, in *Proceedings of the 1987 EPS Conference*, Uppsala, 1987.

[19] C. Jarlskog, Phys. Rev. Lett. **55**, 1039 (1985) and Zeit. Phys. C **29**, 491 (1985).

[20] C. S. Kim, J. L. Rosner, C.-P. Yuan, Phys. Rev. D **42**, 96 (1990).

[21] L. Wolfenstein, Phys. Rev. Lett. **51**, 1945 (1984).

[22] J. Ellis and G. L. Fogli, Phys. Lett. B **232**, 139 (1989); P. Langacker, Phys. Rev. Lett. **63**, 1920 (1989); V. Barger, J. L. Hewett and T. G. Rizzo, Phys. Rev. Lett. **65**, 1313 (1990); J. L. Rosner, Phys. Rev. D **42**, 3107 (1990).

[23] H. Harari and Y. Nir, Nucl. Phys. B **292**, 251 (1987).

[24] C. Jarlskog, Phys. Rev. D **35**, 1685 (1987); D **36**, 2138 (1987); C. Jarlskog and A. Kleppe, Nucl. Phys. B **286**, 245 (1987).

[25] S. J. Parke and T. P. Walker, Phys. Rev. Lett. **57**, 2322 (1986).

[26] J. N. Bahcall and W. C. Haxton, Phys. Rev. D **40**, 931 (1989).

[27] V. N. Gavrin, in Proceedings of the XXV International Conference on High Energy Physics, Singapore (1990).

[28] E. W. Kolb, M. S. Turner and T. P. Walker, Phys. Lett. **175B**, 478 (1986); S. P. Rosen and S. M. Gelb, Phys. Rev. D **34**, 969 (1986); J. N. Bahcall and H. A. Bethe, Phys. Rev. Lett. **65**, 2233 (1990).

[29] N. Ushida et al., Phys. Rev. Lett. **57**, 2897 (1986).

[30] F. Dydak et al., Phys. Lett. B **134**, 281 (1984).

Figure Captions

Figure 1: Contours in the A_N/C_N vs. B_N/C_N plane for fixed values of $|V_{12}|^2$ as indicated. The closely-spaced dotted curve defines the region in which the hierarchical conditions of Eq. (3.10) are satisfied.

Figure 2: IsoSNU contours calculated by Parke and Walker for the gallium experiments superimposed on the allowed MSW region indicated by the closely-space dotted points. The vertical dotted line marks the lower bound on $\sin^2 2\theta_{12}$ found in our model. The cross indicates the point obtained by the parameter set (3.8d) when constrained to the nonadiabatic MSW region by an appropriate choice of heavy Majorana masses.

Figure 3: Contours in the δm^2_{23} vs. $\sin^2 2\theta_{23}$ plane for fixed δm^2_{12} and $|V_{12}|^2 \sim 0.25 \sin^2 2\theta_{12}$ in the nonadiabatic MSW region, with the ratios A_N/C_N and B_N/C_N and the heavy Majorana masses varying along the curves. The Majorana masses are scaled according to the convention given in (3.12) with $\delta m^2_{12} = 2.06 \times 10^{-6}$ eV^2 and $|V_{12}|^2 = 0.00485$ in (a) and $\delta m^2_{12} = 2.0 \times 10^{-7}$ eV^2 and $|V_{12}|^2 = 0.05$ in (b). The allowed regions lie between the dotted curves representing lower bounds for a reasonable hierarchy of parameters stated in (3.10) and the closely-spaced dotted curves representing the upper bounds from the E531 and CDHSW experiments. The crosses indicate the points obtained by the parameter set (3.8d) when constrained to the nonadiabatic MSW region by appropriate choices of heavy Majorana masses.

Figure 4: Scatter plots in (a) the δm^2_{23} vs. $\sin^2 2\theta_{23}$ and (b) δm^2_{13} vs. $\sin^2 2\theta_{13}$ planes obtained by rotating the diagonal $\mathbf{D}_M$ matrices in (3.12) through Euler angles

chosen by 5000 sets of Monte Carlo throws for each point indicated by a cross in (a) lying on the curves in Fig. 3(a). The points indicated by cross potents in (a) remain unchanged by rotations of $\mathbf{D}_M$'s proportional to the identity. The solid curves represent the present experimental upper limits, while the dot-dashed curve in (a) now corresponds to the hierarchical lower bound in Fig. 3(a). Points A and B refer to the special cases discussed in the text. For comparison only, the mixing angle suggested by the recent experiments claiming to see a 17 keV neutrino in their data is indicated by the arrow in (b).

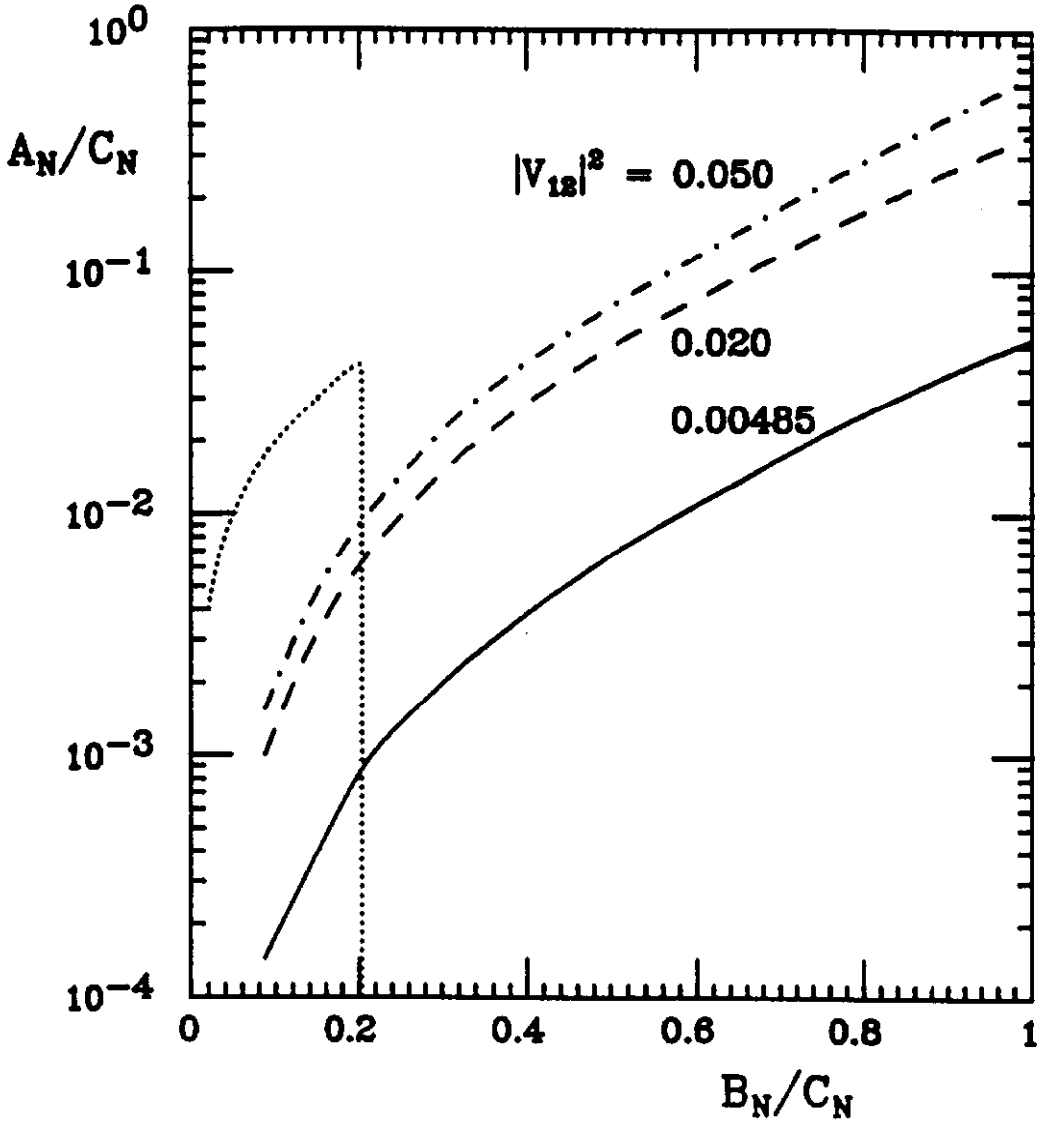
10^0
A_N/C_N
$|V_{12}|^2 = 0.050$
10^{-1}
0.020
0.00485
10^{-2}
10^{-3}
10^{-4}
0
0.2
0.4
0.6
0.8
1
B_N/C_N

Fig. 1

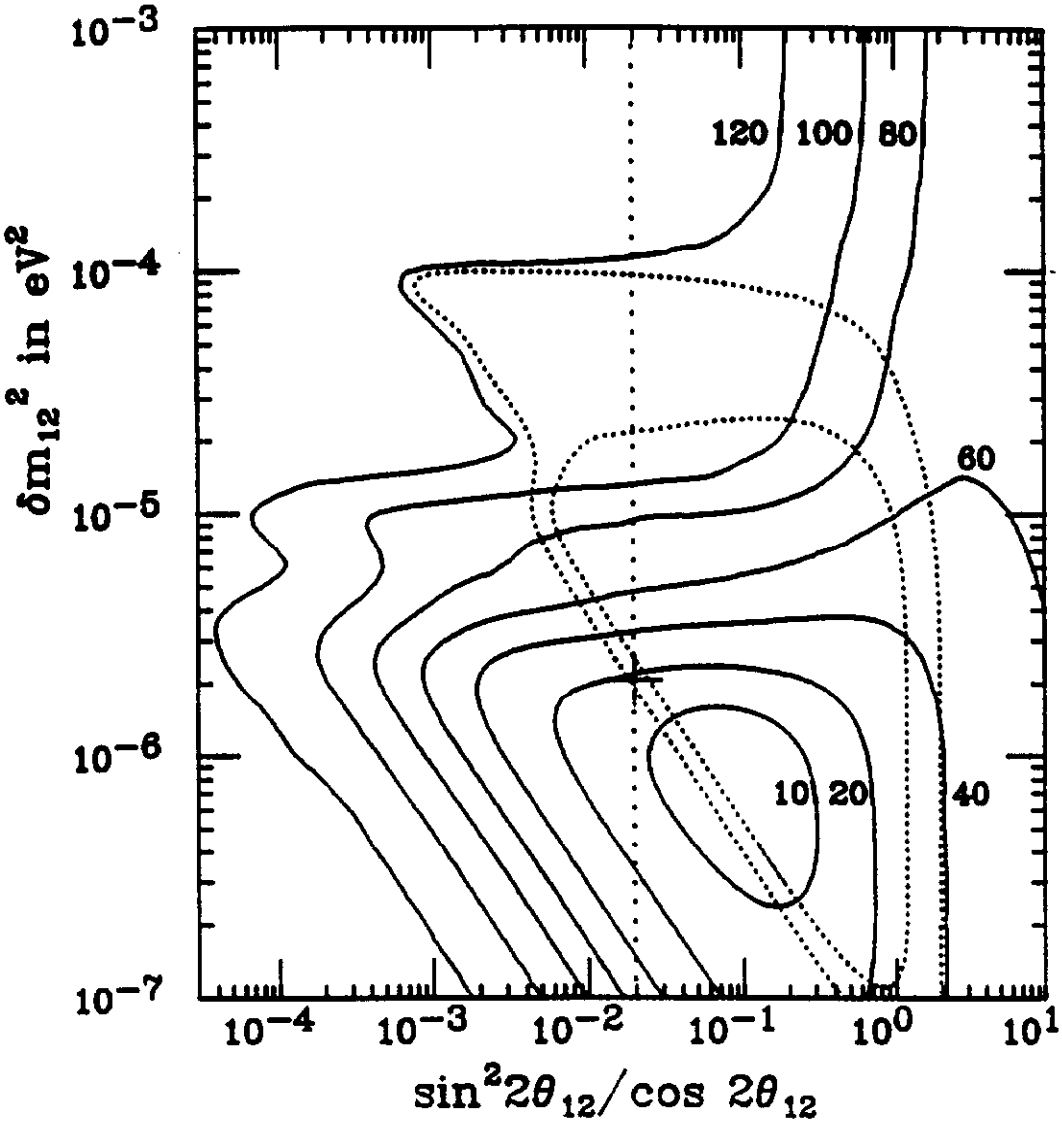
10^{-3}
10^{-4}
10^{-5}
10^{-6}
10^{-7}
δm_{12}^2 in eV^2
120
100
80
60
10
20
40
10^{-4}
10^{-3}
10^{-2}
10^{-1}
10^{0}
10^{1}
$\sin^2 2\theta_{12}/\cos 2\theta_{12}$

Fig. 2

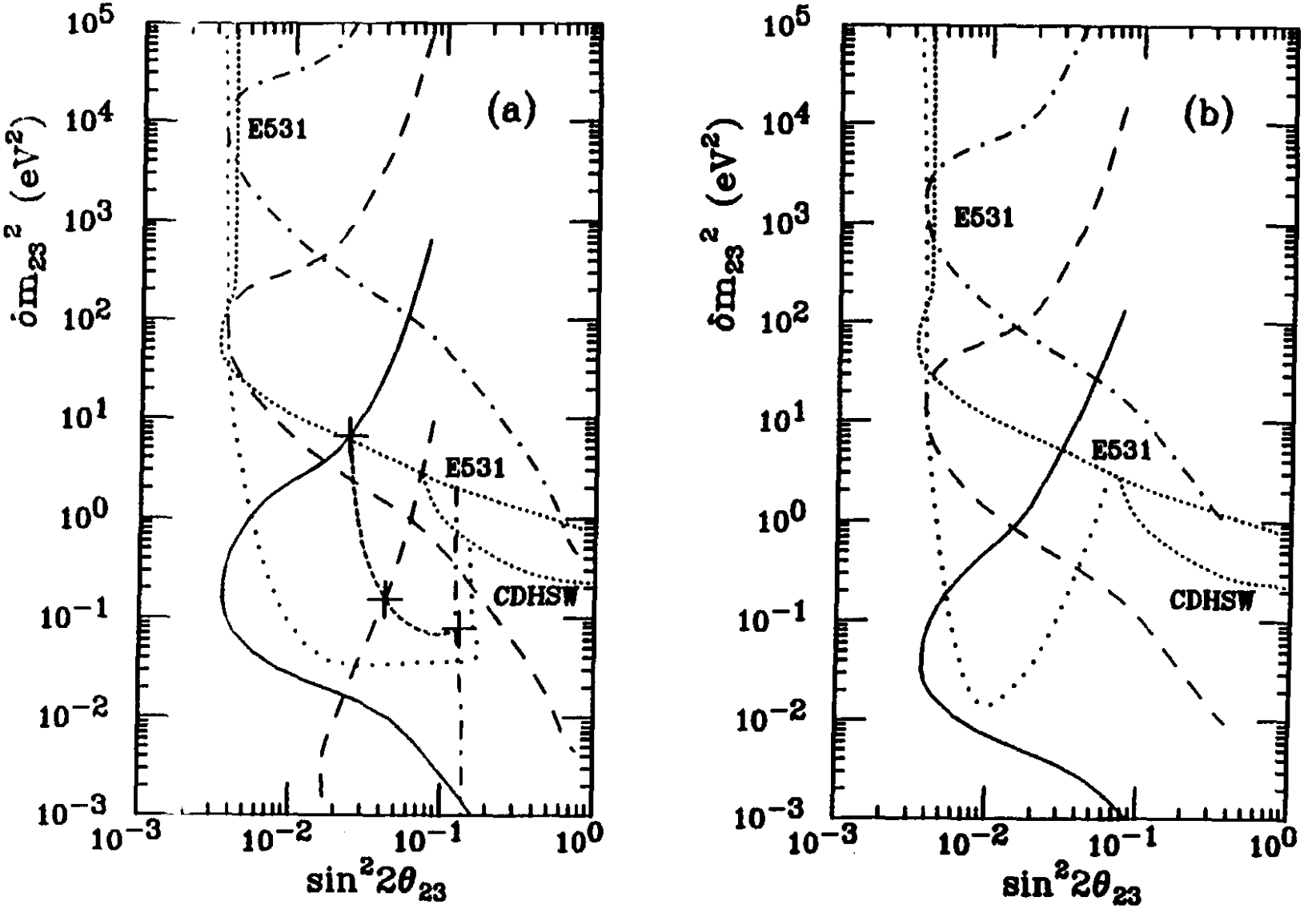
(a)
(b)
E531
E531
E531
CDHSW
CDHSW
δm_{23}^2 (eV^2)
$\sin^2 2\theta_{23}$
10^5
10^4
10^3
10^2
10^1
10^0
10^{-1}
10^{-2}
10^{-3}

Fig. 3

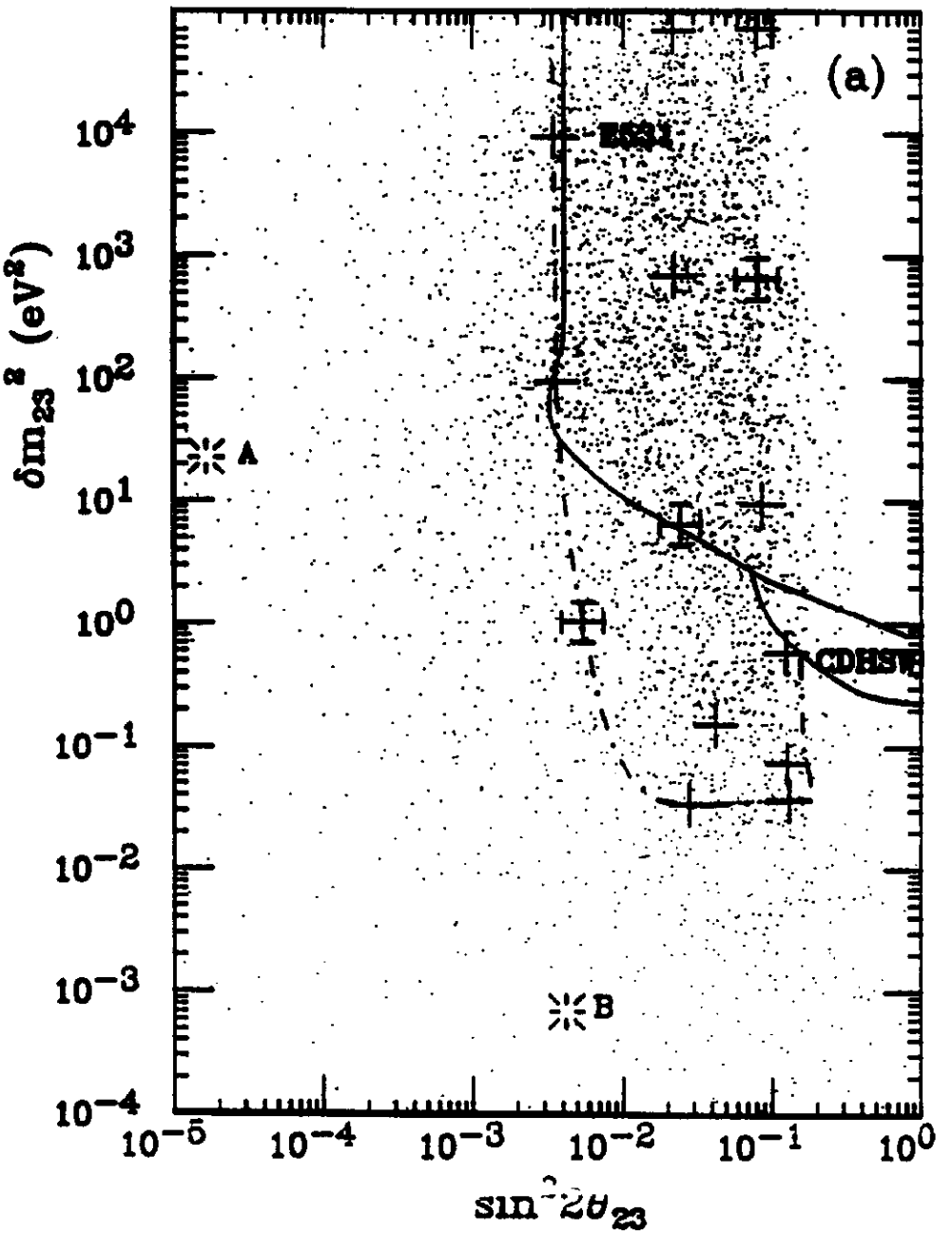
(a)
E531
CDHSW
A
B
10^4
10^3
10^2
10^1
10^0
10^{-1}
10^{-2}
10^{-3}
10^{-4}
δm_{23}^2 (eV^2)
10^{-5}
10^{-4}
10^{-3}
10^{-2}
10^{-1}
10^0
$\sin^2 2\theta_{23}$

Fig. 4

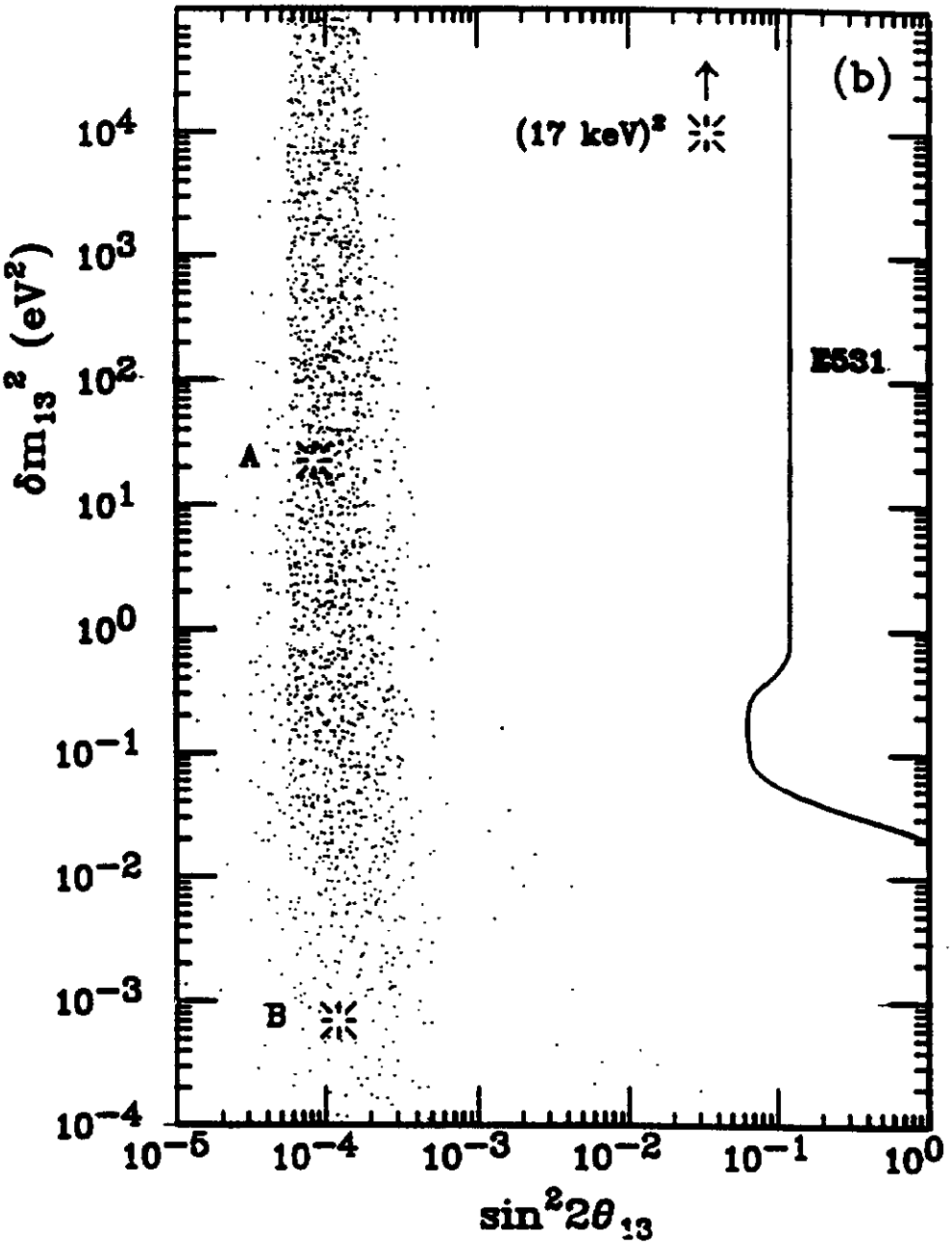
(b)
(17 keV)²
E531
A
B
δm_{13}^2 (eV²)
$\sin^2 2\theta_{13}$
10^4
10^3
10^2
10^1
10^0
10^{-1}
10^{-2}
10^{-3}
10^{-4}
10^{-5}
10^{-4}
10^{-3}
10^{-2}
10^{-1}
10^0

Fig. 4